Hydrol. Earth Syst. Sci. Discuss., https://doi.org/10.5194/hess-2019-42
Manuscript under review for journal Hydrol. Earth Syst. Sci.
Discussion started: 19 March 2019

Hydrology and Earth System Sciences
Open Access
EGU
Discussions

Assessing the impacts of reservoirs on the downstream flood frequency by coupling the effect of the scheduling-related multivariate rainfall into an indicator of reservoir effects

Bin Xiong[1], Lihua Xiong[1*], Jun Xia[1], Chong-Yu Xu[1, 3], Cong Jiang[2], Tao Du[4]

1. State Key Laboratory of Water Resources and Hydropower Engineering Science, Wuhan University, Wuhan 430072, P.R. China

2. School of Environmental Studies, China University of Geosciences (Wuhan), Wuhan 430074, China

3. Department of Geosciences, University of Oslo, P.O. Box 1022 Blindern, N-0315 Oslo, Norway

4. Bureau of Hydrology, Changjiang Water Resources Commission, Wuhan 430010, China

** Corresponding author:*

Lihua Xiong, PhD, Professor

State Key Laboratory of Water Resources and Hydropower Engineering Science

Wuhan University, Wuhan 430072, P.R. China

E-mail: xionglh@whu.edu.cn

Telephone: +86-13871078660

Fax: +86-27-68773568

Hydrol. Earth Syst. Sci. Discuss., https://doi.org/10.5194/hess-2019-42
Manuscript under review for journal Hydrol. Earth Syst. Sci.
Discussion started: 19 March 2019

Hydrology and Earth System Sciences
Open Access
EGU
Discussions

Abstract:

Many studies have shown that the downstream flood regimes have been significantly altered by upstream reservoir operation. Reservoir effects on the downstream flow regime are normally carried out by comparing the pre-dam and post-dam frequencies of some streamflow indicators such as floods and droughts. In this paper, a rainfall-reservoir composite index (RRCI) is developed to precisely quantify reservoir impacts on downstream flood frequency under the framework of covariate-based flood frequency analysis. The RRCI is derived from both the reservoir index (RI) of the previous study and the joint cumulative probability (JCP) of multiple rainfall variables (i.e., the maximum, intensity, volume and timing) of multiday rainfall input (MRI), and is calculated by a c-vine copula model. Then, using RI or RRCI as covariate, a nonstationary generalized extreme value (NGEV) distribution model with time-varying location and/or scale parameters is developed and used to analyze the annual maximum daily flow (AMDF) of Ankang, Huangjiagang and Huangzhuang gauging stations of the Hanjiang River, China with the Bayesian estimation method. The results show that regardless of using RRCI or RI, nonstationary flood frequency analysis demonstrates that the overall flood risk of the basin has been significantly reduced by reservoirs, and the reduction increases with the reservoir capacity. What's more, compared with RI, RRCI through incorporating the effect of the scheduling-related multivariate MRI can better explain the alteration of AMDF. And for a given reservoir capacity (i.e., a specific RI), the flood risk (e.g., the Huangzhuang station) increases with the JCP of rainfall variables and gradually approaches the risk of no reservoir (i.e., RI=0). This analysis, combining the reservoir

39 index with the scheduling-related multivariate MRI to account for the alteration in flood frequency,
40 provides a comprehensive approach and knowledge for downstream flood risk management under the
41 impacts of reservoirs.

42 **Keywords**: Nonstationary; reservoir; flood frequency analysis; multiday rainfall; generalized
43 extreme value distribution; the Hanjiang River

44 1 Introduction

45 River floods are generated by various complex nonlinear processes involving physical factors
46 including "hydrological pre-conditions (e.g. soil saturation, snow cover), meteorological conditions (e.g.
47 amount, intensity, and spatial and temporal distribution of rainfall), runoff generation processes as well
48 as river routing (e.g. superposition of flood waves in the main river and its tributaries)" (Nied et al.,
49 2013; Wyżga et al., 2016). In the absence of reservoirs, a nature extreme flow at the site is directly
50 related to the extreme rainfall in the drainage area. However, after the construction of large or medium-
51 sized reservoirs, the downstream extreme flow is the result of the reservoir scheduling mainly based on
52 reservoir capacity and inflow processes. In recent years, because of its importance for the risk
53 assessment of downstream floods, the study of flood frequency under the impacts of reservoirs has
54 received increasing attention. For example, Benito and Thorndycraft (2005) reported various significant
55 changes of the pre- and post-dam hydrologic regimes (e.g., minimum and maximum flows over
56 different durations) across the United States.

For conventional or stationary frequency analysis to be used in assessing the impact of dams on downstream flood regimes, a basic hypothesis is that hydrologic time series keeps stationarity, i.e., "free of trends, shifts or periodicity (cyclicity)" (Salas, 1993). However, in many cases, changing flooding regimes and the nonstationarity of observed flood series have demonstrated that this strict assumption is invalid (Kwon et al., 2008; Milly et al., 2008). Nonstationarity in the flood regimes downstream of dams makes frequency analysis more complicate. Actually, the frequency of floods downstream of dams is closely related to both climate variability and upstream flood operation. In recent years, there are a lot of attempts linking flood generating mechanisms and reservoir operation to the frequency of flood variable (Gilroy and Mccuen, 2012; Goel et al., 1997; Lee et al., 2017; Liang et al., 2017; Su and Chen, 2018; Yan et al., 2016).

Previous studies have meaningfully increased knowledge related to the reservoir-induced nonstationarity of downstream hydrological extreme frequency (Ayalew et al., 2013; López and Francés, 2013; Liang et al., 2017; Magilligan and Nislow, 2005; Su and Chen, 2018; Wang et al., 2017; Zhang et al., 2015). There are two main approaches to incorporate the effects of reservoirs into flood frequency analysis: the hydrological model simulation approach and the nonstationary frequency modeling approach. In the first approach, a simulating regulated flood time series for the regulated frequency analysis is available by three model components, i.e., stochastic rainfall generator the rainfall-runoff model and the reservoir flood operation module (e.g., reservoir storage capacity, the size of release structures and operation rules). However, as indicated by Ayalew et al. (2013), many simplifying

76 assumptions of this method is suitable just for small single reservoirs; for large single reservoirs or
77 reservoir systems, first approach would fail; besides, a lot of detailed information related to reservoir
78 flood operation module, especially for reservoir systems, may not be available. For this reason, our
79 attention is focused on the second method, the nonstationary frequency modeling approach.
80 Nonstationary distribution models have been widely used to deal with nonstationarity of extreme values.
81 In nonstationary distribution models, distribution parameters are expressed as the functions of
82 covariates to determine the conditional distributions of the extreme values. According to extreme value
83 theory, the maxima series can generally be described by the generalized extreme value distribution
84 (GEV). Thus, previous studies have used the nonstationary generalized extreme value distribution
85 (NGEV) to describe nonstationary maxima series. Scarf (1992) modeled the change in the location and
86 scale parameters of GEV over time through power function relationship. Coles (2001) introduced
87 several time-dependent structures (e.g., trend, quadratic and change-point) into the location, scale and
88 shape parameters of GEV. Adlouni et al. (2007) provided a general NGEV model with an improved
89 parameter estimate method. In recent years, “generalized additive models for location, scale and shape”
90 (GAMLSS) was widely used in nonstationary hydrological frequency analysis (Du et al., 2015; Jiang et
91 al., 2014; López and Francés, 2013; Rigby and Stasinopoulos, 2005; Villarini et al., 2009), but GEV is
92 rarely involved in candidate distributions of GAMLSS. In terms of parameter estimation method for
93 nonstationary distribution model, the maximum likelihood (ML) method is the most common parameter
94 estimate method. However, the ML method for NGEV model may diverge when using numerical

95 techniques to solve likelihood function with small sample. Another drawback of the ML method is that
96 it is not convenient to describe the uncertainty of the estimators. Adlouni et al. (2007) developed the
97 generalized maximum likelihood estimation method (GML) and demonstrated that the GML method
98 has better performance than the ML method in their all cases. Ouarda and El - Adlouni (2011)
99 introduced the Bayesian nonstationary frequency analysis. The Bayesian method can directly describe
100 the uncertainty of extreme flood estimates through providing the prior and posterior distributions of the
101 shape parameter which controls the tail behavior of the NGEV.

102 In the nonstationary frequency modeling approach, a dimensionless reservoir index (RI), as an
103 indicator of reservoir effects, was proposed by López and Francés (2013), and it generally is used as
104 covariate for expression of distribution parameters (e.g., location parameter) (Jiang et al., 2014; López
105 and Francés, 2013). Liang et al. (2017) modified the reservoir index by replacing the mean annual
106 runoff in expression of *RI* with the annual runoff, so that the modified reservoir index can reflect the
107 impact of reservoirs on flood extremes under different total inflow conditions each year. However, this
108 improvement doesn't reveal more accurate effects of reservoirs on the downstream floods. In fact, the
109 effects of reservoirs, especially small or medium-sized reservoirs, may be closely related to not only
110 static reservoir capacity, but also dynamic reservoir operation associated with the multiday rainfall input
111 (MRI), not just annual runoff.

112 Therefore, the aim of the study is to develop an indicator of reservoir effects coupling the RI and
113 the effect of the scheduling-related multivariate rainfall (SRMR), named the rainfall-reservoir

Hydrol. Earth Syst. Sci. Discuss., https://doi.org/10.5194/hess-2019-42
Manuscript under review for journal Hydrol. Earth Syst. Sci.
Discussion started: 19 March 2019

114 composite index (RRIC), and then to assess the reservoir effects through a NGEV model with this
115 indicator as covariate. The specific objectives of this study are: (1) to calculate the RRCI to accurately
116 quantify reservoir effects; (2) to compare RRCI with RI through the covariate-based flood frequency
117 analysis; and (3) to quantify downstream flood risks based on the final NGEV model.

118 # 2 Methods

119 To quantify the effects of reservoirs on the frequency of the AMDF series, a three-step
120 framework (Figure 1), termed the covariate-based flood frequency analysis using the RRIC as covariate,
121 is established. In this section, the methods in this framework are introduced. First, RI of the previous
122 literature is presented. Second, based on RI, the RRCI is developed through incorporating the effect of
123 SRMR. And then, the C-vine copula model is used to construct the cumulative distribution function of
124 MRI variables which is treated as the measure function for the effect of SRMR. Fourth and last, the
125 NGEV model with the Bayesian estimation is clarified.

126 ## 2.1 Reservoir index (RI)

127 Intuitively, the larger the reservoir capacity relative to the natural flow of a downstream gauging
128 station, the greater the effect of the reservoir on streamflow regime is possible. To quantify the
129 reservoir-induced alteration to streamflow regime, Batalla et al. (2004) proposed the impounded runoff
130 index (IRI), a ratio of reservoir capacity (C) to (unimpaired) mean annual flow (R_m), indicated as
131 $IRI = C/R_m$. For a single reservoir, the IRI is a good indicator of the extent to which the reservoir alters

Hydrol. Earth Syst. Sci. Discuss., https://doi.org/10.5194/hess-2019-42
Manuscript under review for journal Hydrol. Earth Syst. Sci.
Discussion started: 19 March 2019

streamflow. To analysis the effect of multi-reservior system on the alteration of flood frequency, López and Francés (2013) proposed a dimensionless reservoir index to indicate the effects of reservoirs on the hydrological regimes in a river. The reservoir index (RI) for a gauging station is defined as

$$RI = \sum_{i=1}^{N} \left(\frac{A_i}{A_T} \right) \cdot \left(\frac{C_i}{R_m} \right) \quad (1)$$

where N is the total number of reservoirs upstream of the gauge station, A_i is the total basin area upstream of the i-th reservoir, A_T is the total basin area upstream of the gauge station, C_i is the water storage capability of the i-th reservoir, and R_m is the mean annual runoff at the gauge station. the Eq. (1) indicates that for a reservoir system consisting of small and middle sized reservoirs, the RI of a gauging station is generally less than 1, but for a system with some large reservoirs, e.g., multi-year regulating storage reservoirs, the RI of the gauging station near this system may be close to 1 or higher. In the following subsection, we will develop a new index to indicate the more precise effects of reservoirs on flood regimes.

2.2 Rainfall-reservoir composite index (RRCI)

In addition to reservoir capacity, multiday rainfall input (MRI) is a key initial condition for the scheduling results of the reservoir system. To add the effect of SRMR into the new indicator of reservoir effects, the multiple scheduling-related variables (denoted as $x_1, x_2, ..., x_d$) of the MRI,

Hydrol. Earth Syst. Sci. Discuss., https://doi.org/10.5194/hess-2019-42
Manuscript under review for journal Hydrol. Earth Syst. Sci.
Discussion started: 19 March 2019

Hydrology and Earth System Sciences
Discussions

149 corresponding to the inflows to the reservoir which will be regulated to become downstream flood
150 events, are considered. The extraction procedure of the MRI is detailed in the section 3.2.

151 We propose a new index called rainfall-reservoir composite index (RRIC) for more
152 comprehensively assessing effects of reservoirs on floods by coupling the RI and the effects of SRMR,
153 defined as

154 $$RRCI = \begin{cases} \left(\bar{F}\left(x_1, x_2, \ldots x_d\right)\right)^{(1/RI-1)}, 0 < RI \le 1 \\ RI, RI > 1 \end{cases} \quad (2)$$

155 Where $\bar{F}(\cdot)$ is the measure function for the effects of SRMR. In this study, the OR-joint exceedance
156 probability $P_{MRI}^{\vee}\left(\bigcup_{i=1}^{d}\left(X_i > x_i\right)\right)$ of the multiple scheduling-related variables of the MRI is used as the
157 measure function. The closer the value of $P_{MRI}^{\vee}$ is to 0, the greater impact the MRI, inferring that the
158 reservoir scheduling is more inflexible, so that the resulting downstream flood is possibly greater, and
159 vice versa. The Eq. (2) can be expressed as

160 $$RRCI = \begin{cases} \left(P_{MRI}^{\vee}\left(\bigcup_{i=1}^{d}\left(X_i > x_i\right)\right)\right)^{(1/RI-1)} = \left(1 - F\left(x_1, x_2, \ldots x_d\right)\right)^{(1/RI-1)}, 0 < RI \le 1 \\ RI, RI > 1 \end{cases} \quad (3)$$

161 Where $F(\cdot)$ is the cumulative distribution function. Figure 2 illustrates the relationship in the Eq. (3),
162 which shows that the RRCI is conditional on the joint cumulative frequency of scheduling-related
163 rainfall variables when given the static capability of reservoirs (RI). The expectation of RRCI is as
164 follow

Hydrol. Earth Syst. Sci. Discuss., https://doi.org/10.5194/hess-2019-42
Manuscript under review for journal Hydrol. Earth Syst. Sci.
Discussion started: 19 March 2019

$$E\left(RRI\right)=\int_{\mathbb{R}^d}\left(1-F\left(x_1,x_2,...x_d\right)\right)^{(1/RI-1)}dF\left(x_1,x_2,...x_d\right)=RI \tag{4}$$

In addition, for the OR case, we have

$$P_{MRI}^{\vee}\left(\bigcup_{i=1}^{d}\left(X_i>x_i\right)\right)\geq P_{MRI}^{\vee}\left(X_i>x_i\right) \tag{5}$$

The Eq. (3) and Eq. (5) indicate that for the given MRI, RRCI considering the multivariate MRI will be greater than or equal to RRCI considering the univariate MRI. To give a reasonable RRCI, unrelated rainfall variables should not be incorporated. We use four variables (i.e., extremes, intensities, volumes and timings) of the MRI as candidate variables to construct the *d*-dimensional ($d=1,2,3,4$) distribution for the calculation of RRCI. The identification of the scheduling-related variables from four candidate variables is based on the rank correlation coefficient between RRCI and the magnitude of AMDF. The construction method of *d*-dimensional ($d=2,3,4$) distribution is described in the following subsection.

<Figure 2>

2.3 C-vine Copula model

In this subsection, a c-vine Copula model for the construction of continuous *d*-dimensional distribution $F\left(x_1,x_2,...x_d\right)$ is clarified. The Sklar's theorem (Sklar, 1959) showed that for a continuous *d*-dimensional distribution, one-dimensional margins and dependence structure can be separated, and the dependence can be represented by a copula formula as follows

$$F\left(x_1,x_2,...x_d\left|\boldsymbol{\theta}\right.\right)=C\left(u_1,u_2,...,u_d\left|\boldsymbol{\theta}_c\right.\right),u_i=F_{X_i}\left(x_i\left|\boldsymbol{\theta}_i\right.\right) \tag{6}$$

Hydrol. Earth Syst. Sci. Discuss., https://doi.org/10.5194/hess-2019-42
Manuscript under review for journal Hydrol. Earth Syst. Sci.
Discussion started: 19 March 2019

Hydrology and Earth System Sciences
Discussions

where $F_{X_i}(\cdot)$ is the univariate marginal distribution of X_i; $C(\cdot)$ is the copula function. $\boldsymbol{\theta}_c$ is the copula parameter vector; $\boldsymbol{\theta}_i$ is the parameter vector of the corresponding margins. $\boldsymbol{\theta}=(\boldsymbol{\theta}_c,\boldsymbol{\theta}_1,\boldsymbol{\theta}_2,...,\boldsymbol{\theta}_d)$ is the parameter vector of the whole *n*-dimensional distribution. Thus, the construction of $F(x_1,x_2,...x_d)$ can be separated into two steps: first is the modeling of the univariate margins; second is the modeling of the dependence structure. For the first step, we use the empirical distribution as univariate marginal distributions. Then, for the second step, the copula construction for dependence modeling is based on the pair-copula construction method which has been widely used in the previous research (Aas et al., 2009; Xiong et al., 2015). According to Aas et al. (2009), the joint density function $f(x_1,x_2,...,x_d)$ is written as

$$f(x_1,x_2,...,x_d|\boldsymbol{\theta})=c_{1...n}(u_1,u_2,...,u_d|\boldsymbol{\theta}_c)\prod_{i=1}^{d}f_{X_i}(x_i|\boldsymbol{\theta}_i),u_i=F_{X_i}(x_i|\boldsymbol{\theta}_i) \quad (7)$$

and the *n*-dimension copula density $c_{1...d}(u_1,u_2,...,u_d)$, which can be decomposed into $d(d-1)/2$ bivariate copulas, corresponding to a c-vine structure, is given by

$$c_{1...d}(u_1,u_2,...,u_d|\boldsymbol{\theta}_c)=\prod_{j=1}^{d-1}\prod_{i=1}^{d-j}c_{j,i+j|1,...,j-1}\left(F(u_j|u_1,...,u_{j-1}),F(u_{i+j}|u_1,...,u_{j-1})\middle|\boldsymbol{\theta}_{j,i|1,...,j-1}\right) \quad (8)$$

where $c_{j,i+j|1,...,j-1}$ is the density function of a bivariate pair copula and $\boldsymbol{\theta}_{j,i|1,...,j-1}$ is a parameter vector of the corresponding bivariate pair copula. And the marginal conditional distribution is

Hydrol. Earth Syst. Sci. Discuss., https://doi.org/10.5194/hess-2019-42
Manuscript under review for journal Hydrol. Earth Syst. Sci.
Discussion started: 19 March 2019

$$F\left(u_{i+j}\left|u_1,...,u_{j-1}\right.\right)=$$
$$\frac{\partial C_{i+j,j-1|1,...,j-2}\left(F\left(u_{i+j}\left|u_1,...,u_{j-2}\right.\right),F\left(u_{j-1}\left|u_1,...,u_{j-2}\right.\right)\left|\boldsymbol{\theta}_{i+j,j-1|u_1,...,u_{j-2}}\right.\right)}{\partial F\left(u_{j-1}\left|u_1,...,u_{j-2}\right.\right)}, \quad (9)$$
$$j=2,...,d-1;\ i=0,...,n-j$$

where $C_{i+j,j-1|1,...,j-2}$ is a bivariate copula distribution function. The maximum dimensionality covered in this study is four. Thus for the four-dimension copula (of which the decomposition is shown in Figure 3), the general expression of Eq. (8) is

$$\begin{aligned}&c_{1234}\left(u_1,u_2,u_3,u_4\left|\boldsymbol{\theta}_c\right.\right)=c_{12}\left(u_1,u_2\left|\boldsymbol{\theta}_{12}\right.\right)c_{13}\left(u_1,u_3\left|\boldsymbol{\theta}_{13}\right.\right)c_{14}\left(u_1,u_4\left|\boldsymbol{\theta}_{14}\right.\right)\cdot\\&c_{23|1}\left(F\left(u_2\left|u_1\right.\right),F\left(u_2\left|u_1\right.\right)\left|\boldsymbol{\theta}_{23|1}\right.\right)c_{24|1}\left(F\left(u_2\left|u_1\right.\right),F\left(u_4\left|u_1\right.\right)\left|\boldsymbol{\theta}_{24|1}\right.\right)\cdot\\&c_{34|12}\left(F\left(u_3\left|u_1,u_2\right.\right),F\left(u_4\left|u_1,u_2\right.\right)\left|\boldsymbol{\theta}_{34|1}\right.\right)\end{aligned} \quad (10)$$

<Figure 3>

2.4 Nonstationary generalized extreme value distribution model with the Bayesian estimation

The covariate-based extreme frequency analysis is extensively concerned and used (Villarini et al., 2009; Ouarda and El‐Adlouni, 2011; López and Francés, 2013; Xiong et al., 2018). In this subsection, the NGEV model based on Bayesian estimation is developed for flood frequency analysis, following Adlouni et al. (2007) and Ouarda and El‐Adlouni (2011).

Suppose that flood variable Y_t obeys nonstationary distribution $f_{Y_t}\left(y_t\left|\boldsymbol{\eta}_t\right.\right)$ with parameters $\boldsymbol{\eta}_t=[\mu_t,\sigma_t,\xi_t]$. This allows stationary frequency analysis to be incorporated into our framework, because the procedure of model selection can identify whether the location, scale and shape parameters

Hydrol. Earth Syst. Sci. Discuss., https://doi.org/10.5194/hess-2019-42
Manuscript under review for journal Hydrol. Earth Syst. Sci.
Discussion started: 19 March 2019

change with the covariates. If they are constants, this process will be stationary frequency analysis. In this study, the flood estimate of NGEV using the RRCI as covariate will be compared with the one using the RI. Considering that the shape parameter is sensitive to quantile estimation of rare events (more details about the shape parameter are referred in the section of parameter estimation), only location and scale parameters are allowed to vary with covariates. Thus, a nonstationary GEV density function is given by:

$$f_{Y_t}\left(y_t\left|\mu_t,\sigma_t,\xi_0\right.\right)=\frac{1}{\sigma_t}\left[1+\xi_0\left(\frac{y_t-\mu_t}{\sigma_t}\right)\right]^{-1/\xi_0-1}\exp\left\{-\left[1+\xi_0\left(\frac{y_t-\mu_t}{\sigma_t}\right)\right]^{-1/\xi_0}\right\} \quad (11)$$
$$-\infty<\mu_t<\infty,\sigma_t>0,-\infty<\xi_0<\infty$$

According to the linear additive formulation of Generalized Additive Models for Location, Scale, and Shape (GAMLSS) (Rigby and Stasinopoulos, 2005; Villarini et al., 2009), the NGEV models with different formula of the location and scale parameters are show in Table 1.

<Table 1>

Take the model $\mathrm{NGEV}(\mu_t \sim \mathrm{RRCI}, \sigma_t \sim \mathrm{RRCI})$ as an example, the parameter vector $\boldsymbol{\theta}_{\mathrm{NGEV}}=\left[\mu_0,\mu_1,\sigma_0,\sigma_1,\xi_0\right]$ is to be estimate. We use the Bayesian method to estimate $\boldsymbol{\theta}_{\mathrm{NGEV}}$. Let the prior probability distribution be $\pi\left(\boldsymbol{\theta}_{\mathrm{NGEV}}\right)$ and observations $\boldsymbol{D}$ have the likelihood $l\left(\boldsymbol{D}\left|\boldsymbol{\theta}_{\mathrm{NGEV}}\right.\right)$, then the posterior probability distribution $p\left(\boldsymbol{\theta}_{\mathrm{NGEV}}\left|\boldsymbol{D}\right.\right)$ can be calculated with Bayes' theorem, as follow

$$p\left(\boldsymbol{\theta}_{\mathrm{NGEV}}\left|\boldsymbol{D}\right.\right)=\frac{l\left(\boldsymbol{D}\left|\boldsymbol{\theta}_{\mathrm{NGEV}}\right.\right)\pi\left(\boldsymbol{\theta}_{\mathrm{NGEV}}\right)}{\int_{\Omega}l\left(\boldsymbol{D}\left|\boldsymbol{\theta}_{\mathrm{NGEV}}\right.\right)\pi\left(\boldsymbol{\theta}_{\mathrm{NGEV}}\right)d\boldsymbol{\theta}_{\mathrm{NGEV}}}\propto l\left(\boldsymbol{D}\left|\boldsymbol{\theta}_{\mathrm{NGEV}}\right.\right)\pi\left(\boldsymbol{\theta}_{\mathrm{NGEV}}\right) \quad (12)$$

Hydrol. Earth Syst. Sci. Discuss., https://doi.org/10.5194/hess-2019-42
Manuscript under review for journal Hydrol. Earth Syst. Sci.
Discussion started: 19 March 2019

Hydrology and Earth System Sciences
Discussions

where the integral is the normalizing constant and $\boldsymbol{\Omega}$ is the whole parameter space. The obvious difference between the Bayesian method and the frequentist method is that Bayesian method considers the parameters $\boldsymbol{\theta}_{\mathrm{NGEV}}$ to be random variables, and the desired distribution of the random variables can be obtained by a Markov chain which can constructed by using various Monte Carlo (MCMC) algorithms (Reis Jr and Stedinger, 2005; Ribatet et al., 2007) to process Eq. (12). And in this study, we use the Metropolis-Hastings algorithm (Chib and Greenberg, 1995; Viglione et al., 2013), which can be done by aid of the R package "MHadaptive" (Chivers, 2012). We use a beta distribution function with the parameters $u=6$ and $v=9$, which is suggested by Martins and Stedinger (2000); Martins and Stedinger (2001), as the prior distribution on the shape parameter ξ_0. For the other parameters $\mu_0, \mu_1, \sigma_0, \sigma_1$, the prior distributions are set to non-informative (flat) priors. There are two advantage of the Bayesian method. First, as noted by Adlouni et al. (2007), this method allows the addition of the other information, e.g., historical and regional information, through defining the prior distribution. Second, the Bayesian method can provide an explicit way to account for the uncertainty of flood estimation. In nonstationary case, in the *t*-year, the 95% credible interval for the estimation of the flood quantile corresponding to a given probability p can be obtained from a set of stable parameters estimations $\hat{\boldsymbol{\theta}}^{i}_{\mathrm{NGEV}}(i=1,2,...,M_c)$ in which M_c is the length of the Markov chain.

The Akaike's information criterion (AIC) (Akaike, 1974) is used to rank the performance of the NGEV models shown in Table 1, which is given by

Hydrol. Earth Syst. Sci. Discuss., https://doi.org/10.5194/hess-2019-42
Manuscript under review for journal Hydrol. Earth Syst. Sci.
Discussion started: 19 March 2019

Hydrology and Earth System Sciences
Discussions

$$AIC = -2\log\mathrm{L}(M) + 2df \tag{13}$$

where $\log\mathrm{L}(M)$ is the maximized log-likelihood of the NGEV model (M) and df is the freedom degree.

In this study, to test the significance of the more complex model structure for nested models, we refer to the chi-square test (Coles, 2001). Given the models $M_0 \subseteq M_1$, the deviance statistic for the test is defined as

$$D = 2\left(\log\mathrm{L}(M_1) - \log\mathrm{L}(M_0)\right) \tag{14}$$

When the p-value of the chi-square distribution χ_k (k is the difference of the number of the parameters between the two models M_0 and M_1) is less than 0.05, the more complex model (M_1) is considered significant. We use the quantile plot based on the diagnosis method suggested by Coles (2001) to check whether the final model can well represent the data. In the nonstationary case, the diagnosis can be performed by testing the standardized series (denoted as $\overline{Y_t}$) of the nonstationary flood series (Y_t), conditional on the fitted parameter values. The variable $\overline{Y_t}$ is defined by

$$\overline{Y_t} = \frac{1}{\xi_0}\ln\left(1+\xi_0\frac{Y_t-\mu_t}{\sigma_t}\right) \tag{15}$$

If the model is correct (i.e., $Y_t \sim GEV(\mu_t, \sigma_t, \xi_0)$), $\overline{Y_t}$ have a standard Gumbel distribution.

3 Study area and data

3.1 Study area

The Hanjiang River (Figure 4), with the coordinates of 30°30′-34°30′ N, 106°00′-114°00′ E and a catchment area of 159000 km^2, is the largest tributary of the Yangtze River, China. Since 1960, many

reservoirs have been completed in the Hanjiang basin. The information of the middle-sized and large reservoirs has been shown in Table 2, including the longitude, latitude, control area, time for completion and capability. The Danjiangkou Reservoir in central China's Hubei province is the largest one in this basin, which is completed by 1967. After the Danjiangkou Dam Extension Project in 2010, the Danjiangkou Reservoir gained an additional capacity of 13.0 billion m^3 and an extra flood control storage capacity of 3.3 billion m^3. Previous studies demonstrated that the effect of reservoirs on the flow regime of the Hanjiang River is significant (Cong et al., 2013; GUO et al., 2008; Jiang et al., 2014; Lu et al., 2009).

<Figure 4>

<Table 2>

3.2 Data

The assessment analysis of reservoir effects on flood frequency utilizes the streamflow data, the reservoir data, and the rainfall data. The annual maximum daily flood series (AMDF) is extracted from the daily streamflow records of the three gauges in the Hanjiang River basin, namely Ankang (AK) station (with a drainage area of 38600 km^2), Huangjiagang (HJG) station (with a drainage area of 90491 km^2) and Huangzhuang (HZ) station (with a drainage area of 142056 km^2). The streamflow and reservoir data are provided by the Hydrology Bureau of the Changjiang Water Resources Commission, China (http://www.cjh.com.cn/en/index.html). Annual series of the maximum (M), mean intensity (I),

Hydrol. Earth Syst. Sci. Discuss., https://doi.org/10.5194/hess-2019-42
Manuscript under review for journal Hydrol. Earth Syst. Sci.
Discussion started: 19 March 2019

281 volume (V) and timing (T) in the annual critical MRI (defined as continuous daily rain records
282 matching the timing of AMDF, and in which any two consecutive days of rainfall values require more
283 than 0.2 mm) are obtained from the areal average daily rainfall series which are calculated using the
284 inverse distance weighting (IDW) method, based on the rainfall records of 16 sites (shown in Figure 4)
285 which are downloaded from the National Climate Center of the China Meteorological Administration
286 (source: http://www.cma.gov.cn/). For the Ankang and Huangzhuang stations, all records are available
287 from 1956 to 2015, while the records of the Huangjiagang station are available from 1956 to 2013.

288 # 4 Results

289 ## 4.1 The identification of the reservoir effects

290 In this section, to confirm the impact of reservoirs on annual maximum daily flow (AMDF) in the study
291 area, the two statistical tests were performed, including the Mann–Kendall test (Kendall, 1975; Mann,
292 1945) for trend component and the Pettitt test (Pettitt, 1979) for change point, and then, the statistical
293 characteristics of AMDF before and after reservoir construction were analyzed. According to the Table
294 3, the mean and standard deviation of flood series in AK, HJG and HZ stations were significantly
295 reduced after reservoir construction. Taking the HJG station as an example, after the completion of two
296 large reservoirs (in 1966 and 1992, respectively), the mean of AMDF (1992-2013) is 4139 m^3/s, which
297 is only 0.28 time of 14951 m^3/s (1956-1966) and the standard deviation is 4074 m^3/s, about 0.52 time of
298 7896 m^3/s (1956-1966). Thus, the results of Table 3 indicate that the impact of reservoirs is significant
299 for floods in the Hanjiang River basin.

<Table 3>

Actually, although the Danjiangkou Reservoir (built in 1967) is a very large reservoir, its construction time and change point of floods series are inconsistent. This could be caused by the effects of other medium-large reservoirs (listed in Table 2) and rainfall factors (e.g., special extreme MRI may limit or reduce the effects of the reservoir). Figure 5 presents the linear correlation between the four variables of the MRI and AMDF. It is found that for the three stations (AK, HJG and HZ), except for the timing (T) of the MRI in the AK station, Pearson correlation coefficients between each rainfall variable and AMDF range from 0.27 to 0.71 (p-value>0.05), indicating that multivariate MRI significantly affects AMDF. The further analysis for more precise effects of reservoirs is performed in the 4.2 and 4.3 sections.

<Figure 5>

4.2 Results for rainfall-reservoir composite index (RRCI)

The C-vine copula model was applied to model the joint probability of the rainfall variables. To identify the scheduling-related rainfall variables (i.e., the best subset from four rainfall variables), the RRCI for all subsets were calculated and compared. The Pearson, Kendall, and Spearman correlation coefficients between RRCI and AMDF are listed in Table 4. In Table 4, the ordering of the root nodes (T1 of C-vine decomposition in Figure 3) determining the whole decomposition structure matches the ordering of variables in the cell of the first column. As shown in the first row of Table 4, there is a negative correlation between AMDF and RI for the AK, HJG and HZ stations. The values of the

319 Pearson correlation coefficient between AMDF and RI for the AK, HJG and HZ stations are -0.36, -
320 0.56 and -0.53, respectively, demonstrating that there is a significant relation between reservoirs
321 capacity and reduction of AMDF. And after introducing the effect of multivariate MRI (measured by the
322 OR-joint exceedance probability $P_{MRI}^{\vee}$ of the variables in MRI) into RRCI, the negative correlation
323 becomes stronger, indicating that RRCI can more accurately represent the impacts of the reservoirs. To
324 derive the RRCI, the rainfall variables are identified as the scheduling-related variables through the
325 highest Kendall correlation. According to the highest Kendall correlation, the scheduling-related
326 variables for the AK station are the maximum, intensity, volume and timing; those for the HJG station
327 are the intensity and timing; and those for the HZ station are the intensity, volume and timing.

328 <Table 4>

329 Table 5 is the results of the final C-vine copula model for modeling the joint distribution of the
330 scheduling-related variables, by aid of the R package "VineCopula" (https://CRAN.R-
331 project.org/package=VineCopula). For each bivariate pair in the third column of Table 5, three one-
332 parameter bivariate Archimedean copula families (i.e., the Gumbel, Frank, and Clayton copulas)
333 (Nelsen, 2006), are used to select from. As shown in Table 5, the results of the Cramer-von Mises test
334 (Genest et al., 2009) show that the C-vine copula model passed the test at the significant level of 0.05,
335 indicating the model can be effective for simulating the joint distribution of the scheduling-related
336 variables. Finally, the change of RI and RRCI over time is displayed in Figure 6. It is found that after
337 reservoir construction, for most years, the values of RRCI are larger (close to 1) than those of RI, which

Hydrol. Earth Syst. Sci. Discuss., https://doi.org/10.5194/hess-2019-42
Manuscript under review for journal Hydrol. Earth Syst. Sci.
Discussion started: 19 March 2019

338 implied that the effects of reservoirs on AMDF in these years may be underestimated by RI. On the
339 other hand, for few special years, because of special rainfall events, the effect of reservoirs on AMDF
340 may be overestimated by RI.

341 <Figure 6>

342 <Table 5>

343 **4.3 Flood frequency analysis**

344 In this section, nonstationary flood frequency analysis using RRCI or RI as covariate is performed to
345 investigate how reservoirs affect the frequency of AMDF. The results of AIC in Table 6 show that for
346 the models (M11, M12 and M13) using RI as covariate, the performance of model (M13) in which both
347 location and scale parameters of GEV distribution are time-varying is better than the models (M11 and
348 M12) in which only location or scale parameter are time-varying. And this situation is the same for the
349 models (M21, M22 and M23) using RRCI as covariate. Thus, to compare RRCI with RI, we only focus
350 on the model M13 and the model M23. Take the HZ station as an example. The time-varying GEV
351 distribution parameters for the HZ station are given as follows

352 (1) Model M13

353

354
$$\begin{aligned} \mu_t &= 9333 - 12257RI \\ \sigma_t &= \exp\left(9.048 - 2.531RI\right) \\ \xi_0 &= 0.099 \end{aligned} \tag{16}$$

Hydrol. Earth Syst. Sci. Discuss., https://doi.org/10.5194/hess-2019-42
Manuscript under review for journal Hydrol. Earth Syst. Sci.
Discussion started: 19 March 2019

355 (2) Model M23

$$\begin{aligned} \mu_t &= 11850 - 8937 RRCI \\ \sigma_t &= \exp\left(9.007 - 1.418 RRCI\right) \\ \xi_0 &= -0.065 \end{aligned} \tag{17}$$

356

357 For the model M13, the estimate values of μ_1 and σ_1 are -12257 and -2.531, respectively, while for the
358 model M23, the estimate values of μ_1 and σ_1 are -8937 and -1.418. The negative estimate values of μ_1
359 and σ_1 in the Eq. (16) and Eq. (17) reveal reduction of both magnitude and scale of AMDF due to the
360 reservoir construction. As shown in Table 6, the best model for each gauging station is M23 with the
361 smallest AIC value, which means that RRCI as covariate is better than RI for explaining the alteration
362 of both location and scale parameters of GEV distribution. The results of the chi-square test in Table 6
363 indicate that the more complex structures of the best models (M23), compared to other models (except
364 for M21 in the AK station) are significant at the significant level of 0.05. The results of parameter
365 estimation of M23 are displayed in Table 7.

366 <Table 6>

367 <Table 7>

368 Figure 7 presents the performance of the best model (M23) for AK, HJG and HZ stations. The points in
369 the quantile-quantile plots of Figure 7 are close to 1:1 lines, indicating that the NGEV model (M23)
370 with RRCI as covariate is a reasonable model. And according to the centile curves plots of Figure 7, the
371 flood series is well fitted by M23 using the covariate RRCI. Take the case of the HZ station. After the
372 construction of Danjiangkou Reservoir (1967), due to flood operation, the magnitude and scale of

floods are significantly reduced. Moreover, considering the limits of the multivariate MRI to flood operation, RRCI well explain the variation characteristics of flood after 1967.

<Figure 7>

The 100-year return levels with the 95% credible interval from the NGEV models (M13 and M23) for the three stations are presented in Figure 8. For each station, compared to M13, M23 provides a lower 100-year return level and a smaller uncertainty range, which means that M13 with RI as covariate may underestimate the effect of reservoirs on the floods. An overestimated return level of M13 is possibly because in most years, the impact of the reservoir indicated by RI is less than that indicated by RRCI considering the multivariate MRI. Further explanation from the perspective of reservoir operation is that weak dependence relationships between the scheduling-related variables of MRI indicated by the Kendall's tau of Table 5 is likely to reduce the flood magnitude during the periods of flood control. Besides, the other advantage for RRCI is that the consideration of the multivariate MRI reduced the uncertainty range of flood estimates.

<Figure 8>

Take the HZ gauging station as an example to illustrate the reservoir effects on the flood risk. We investigate the risk rates (the exceedance probability) of four levels (8000, 12000, 16000 and 20000 m^3/s) corresponding to different flood losses according to the study of DUAN Weixin (2018). Figure 9 presents the risk rates of AMDF from M23 in the 1956-1966 (RI=0), 1967-1992 (RI=0.30), 1992-2012 (RI=0.32), and 2013-future (RI=0.50) periods. First, for every certain multivariate MRI, the risk rate on

each level of flood decreases with the increasing RI. Second, given a non-zero RI, the risk rate on each level of flood increases with the increasing joint cumulative probability of the scheduling-related rainfall variables (i.e., intensity, volume and timing) and gradually approaches the risk of no reservoir effects (RI =0).

<Figure 9>

5 Discussions

Table 8 shows the top 5 floods and related variables after the construction (1966) of Danjiangkou reservoir in the HZ station. It is found that the largest floods of 1967-2015 in the HZ station occurred in 1983. For this flood event, the multiday rainfall input (MRI) can be considered rare ($P_{MRI}^{\vee} = 0.474$ ranking the 3rd) due to the largest mean intensity (20.2 mm) and second late occurrence (the 281th day). It is interest that the timings (ranking 2-6) of the extreme MRI for all of top 5 downstream floods seem to be overall later than those for the ordinary floods. It may be because near the end of the major flood control period (July-October), the remained capacity of reservoir is not sufficient to regulate the inflow floods caused by the late extreme MRI. Therefore, the timing of the extreme MRI may be an important factor for producing the exceptional downstream flood events for the HZ station.

In this study, the multivariate rainfall samples are obtained though corresponding the annual maximum streamflow. This means that some extreme MRI samples due to correspond to non-maximum

410 flow are not included, resulting in the estimation error for $P_{MRI}^{\vee}$. Nonetheless, the good performance of
411 frequency modeling demonstrates these multivariate rainfall samples may still have representativeness.
412 The peaks-over-threshold sampling method would be considered to obtain enough samples in the future
413 study.

414 ## 6 Conclusions

415 We have shown that the regime of downstream floods in the study area was affected by the large
416 reservoirs. The real effect of reservoirs on floods is possibly related to both the reservoir capability and
417 the joint variation of scheduling-related rainfall variables (i.e., the maximum, intensity, volume and
418 timing of the MRI). It is found that the NGEV model using RRCI as covariate can lead to more accurate
419 flood estimations than either that using RI as covariate or the stationary GEV model. The result
420 demonstrates that the consideration of scheduling-related rainfall variables of the MRI is necessary for
421 assessing the impact of reservoirs on flood frequency.

422 Results in the identification of the reservoir effects show that the nonstationarity of AMDF is
423 significant and is possibly related to construction of the two large reservoirs (i.e., Danjiangkou and
424 Ankang reservoirs completed in 1967 and 1992, respectively). This is consistent with the results on the
425 effect of reservoirs on the flow regime in previous literature (Cong et al., 2013; GUO et al., 2008; Jiang
426 et al., 2014; Lu et al., 2009). The results of the C-vine copula show that the dependence relationships
427 between multiple rainfall variables are weak (Table 5). The Comparison between RRCI and RI (Figure
428 6) indicate that to some extent, for the given reservoir capacity, these weak dependency relationships

429 produced higher values of RRCI than that of RI in most case, however, some rare multivariate MRI still
430 would produce lower values of RRCI than that of RI. According to the interannual variation of RRCI,
431 for the downstream stations affected by reservoirs, it is expected to more significantly reduce the
432 number of large floods in most years; meanwhile, some unexpected large floods still will occur
433 conditional on rare high-impact multivariate MRI. Finally, the results of flood frequency analysis
434 demonstrated that as expected, RRCI better explains the interannual variability of AMDF than RI and
435 provided a lower flood estimation of 100-years return level with a smaller uncertainty range.

436 Accurately assessing the impact of reservoirs on downstream floods is an important issue for
437 flood risk management. In this study, to evaluate the more likely effects of reservoirs on downstream
438 flood risk of Hanjiang River, RRCI is derived from Eq. (3) which takes account of a combination of the
439 reservoir index and the joint frequency of scheduling-related rainfall variables. Then, the nonstationary
440 frequency model using RRCI as covariate is developed to obtain flood estimates and risk rates,
441 conditional on both multivariate rainfall frequencies and reservoir index. The flood risk corresponding
442 to a certain level of loss has been reduced by reservoirs; while, given the reservoir index, the flood risk
443 of rare multivariate MRI still is greater than that of ordinary multivariate MRI, but not higher than the
444 flood risk of no reservoir. Thus, during flood control periods, the prediction of multivariate MRI may
445 play an important role in assessing the downstream flood risk. The study provided a comprehensive
446 approach and knowledge for flood risk management to perform more accurate analysis of reservoir
447 effects.

Acknowledgments

This research is financially supported jointly by the National Natural Science Foundation of China (NSFC Grants 41890822 and 51525902), the Research Council of Norway (FRINATEK Project 274310), and the "111 Project" Fund of China (B18037), all of which are greatly appreciated. No conflict of interest exists in the submission of the manuscript.

References

Aas, K., Czado, C., Frigessi, A., Bakken, H., 2009. Pair-copula constructions of multiple dependence. Insurance: Mathematics and Economics, 44(2): 182-198. https://doi.org/10.1016/j.insmatheco.2007.02.001

Adlouni, S.E., Ouarda, T.B.M.J., Zhang, X., Roy, R., Bobée, B., 2007. Generalized maximum likelihood estimators for the nonstationary generalized extreme value model. Water Resources Research, 43(3): 455-456. https://doi.org/10.1029/2005WR004545.

Akaike, H., 1974. A new look at the statistical model identification. IEEE Transactions on Automatic Control, 19(6): 716-723. https://doi.org/10.1109/TAC.1974.1100705.

Ayalew, T.B., Krajewski, W.F., Mantilla, R., 2013. Exploring the effect of reservoir storage on peak discharge frequency. Journal of Hydrologic Engineering, 18(12): 1697-1708. https://doi.org/10.1061/(ASCE)HE.1943-5584.0000721.

Batalla, R.J., Gomez, C.M., Kondolf, G.M., 2004. Reservoir-induced hydrological changes in the Ebro River basin (NE Spain). Journal of Hydrology, 290(1-2): 117-136. https://doi.org/10.1016/j.jhydrol.2003.12.002

Benito, G., Thorndycraft, V.R., 2005. Palaeoflood hydrology and its role in applied hydrological sciences. Journal of Hydrology, 313(1–2): 3-15. https://doi.org/10.1016/j.jhydrol.2005.02.002.

Chib, S., Greenberg, E., 1995. Understanding the metropolis-hastings algorithm. The American Statistician, 49(4): 327-335. https://doi.org/10.1080/00031305.1995.10476177.

Chivers, C., 2012. MHadaptive: General Markov Chain Monte Carlo for Bayesian Inference using adaptive Metropolis-Hastings sampling. https://CRAN.R-project.org/package=MHadaptive

Coles, S., 2001. An introduction to statistical modeling of extreme values. https://doi.org/10.1007/978-1-4471-3675-0

Cong, M., Chunxia, L., Yiqiu, L., 2013. Runoff change in the lower reaches of Ankang Reservoir and the influence of Ankang Reservoir on its downstream. Resources and Environment in the Yangtze Basin, 22(11): 1433-1440.

Du, T. et al., 2015. Return period and risk analysis of nonstationary low-flow series under climate change. Journal of Hydrology, 527: 234-250. https://doi.org/10.1016/j.jhydrol.2015.04.041

DUAN Weixin, G.S., ZHANG Jun, XING Wenhui, BA Huanhuan, 2018. Study on dynamic control scheme of water level of Danjiangkou Reservoir during flood season. Yangtze River, 49(1): 7-12.

Genest, C., Rémillard, B., Beaudoin, D., 2009. Goodness-of-fit tests for copulas: A review and a power study. Insurance: Mathematics and Economics, 44(2): 199-213. https://doi.org/10.1016/j.insmatheco.2007.10.005

Gilroy, K.L., Mccuen, R.H., 2012. A nonstationary flood frequency analysis method to adjust for future climate change and urbanization. Journal of Hydrology, s 414–415(2): 40-48. https://doi.org/10.1016/j.jhydrol.2011.10.009

Goel, N.K., Kurothe, R.S., Mathur, B.S., Vogel, R.M., 1997. A derived flood frequency distribution for correlated rainfall intensity and duration. Water Resources Research, 33(9): 2103–2107. https://doi.org/10.1029/97WR00812

GUO, W.-x., XIA, Z.-q., WANG, Q., 2008. Effects of Danjiangkou Reservoir on hydrological regimes in the middle and lower reaches of Hanjiang River. Journal of Hohai University (Natural Sciences), 36(6): 733-737. https://doi.org/10.3876/j.issn.1000-1980.2008.06.002

Jiang, C., Xiong, L., Xu, C.Y., Guo, S., 2014. Bivariate frequency analysis of nonstationary low-flow series based on the time-varying copula. Hydrological Processes, 29(6): 1521-1534. https://doi.org/10.1002/hyp.10288

Kendall, M.G., 1975. Rank Correlation Methods, Griffin, Londom.

Kwon, H.-H., Brown, C., Lall, U., 2008. Climate informed flood frequency analysis and prediction in Montana using hierarchical Bayesian modeling. Geophysical Research Letters, 35(5). https://doi.org/10.1029/2007GL032220

López, J., Francés, F., 2013. Non-stationary flood frequency analysis in continental Spanish rivers, using climate and reservoir indices as external covariates. Hydrology and Earth System Sciences, 17(8): 3189-3203. https://doi.org/10.5194/hess-17-3189-2013

Lee, J., Heo, J.-H., Lee, J., Kim, N., 2017. Assessment of Flood Frequency Alteration by Dam Construction via SWAT Simulation. Water, 9(4): 264. https://doi.org/10.3390/w9040264

508 Liang, Z. et al., 2017. A sample reconstruction method based on a modified reservoir index for
509 flood frequency analysis of non-stationary hydrological series. Stochastic Environmental Research and
510 Risk Assessment: 1-11. https://doi.org/10.1007/s00477-017-1465-1

511 Lu, G.-b., Liu, Y., Zou, X.-l., Zou, Z.-h., Cai, T., 2009. Impact of the Danjiangkou Reservoir on
512 the flow regime in the middle and lower reaches of Hanjiang River. Resources and Environment in the
513 Yangtze Basin, 18(10): 959-963.

514 Magilligan, F.J., Nislow, K.H., 2005. Changes in hydrologic regime by dams. Geomorphology,
515 71(1-2): 61-78. https://doi.org/10.1016/j.geomorph.2004.08.017

516 Mann, H.B., 1945. Nonparametric Tests Against Trend. Econometrica, 13(3): 245-259.

517 Martins, E.S., Stedinger, J.R., 2000. Generalized maximum-likelihood generalized extreme-value
518 quantile estimators for hydrologic data. Water Resources Research, 36(3): 737-744.
519 https://doi.org/10.1029/1999WR900330

520 Martins, E.S., Stedinger, J.R., 2001. Generalized maximum likelihood Pareto-Poisson estimators
521 for partial duration series. Water Resources Research, 37(10): 2551-2557.

522 Milly, P.C.D. et al., 2008. Stationarity Is Dead: Whither Water Management? Science, 319(5863):
523 573-4. https://doi.org/10.1029/2001WR000367

524 Nelsen, R., 2006. An Introduction to Copulas . NY: Springer Science+ Business Media. Inc.
525 https://doi.org/10.1007/0-387-28678-0

526 Nied, M., Hundecha, Y., Merz, B., 2013. Flood-initiating catchment conditions: a spatio-temporal
527 analysis of large-scale soil moisture patterns in the Elbe River basin. Hydrology and Earth System
528 Sciences, 17(4): 1401-1414. https://doi.org/10.5194/hess-17-1401-2013

529 Ouarda, T., and S. El - Adlouni (2011), Bayesian nonstationary frequency analysis of
530 hydrological variables 1, JAWRA Journal of the American Water Resources Association, 47(3), 496-
531 505. https://doi.org/10.1111/j.1752-1688.2011.00544.x

532 Pettitt, A.N., 1979. A Non-Parametric Approach to the Change-Point Problem. Journal of the
533 Royal Statistical Society, 28(2): 126. https://www.jstor.org/stable/2346729

534 Reis Jr, D.S., Stedinger, J.R., 2005. Bayesian MCMC flood frequency analysis with historical
535 information. Journal of hydrology, 313(1-2): 97-116. https://doi.org/10.1016/j.jhydrol.2005.02.028

536 Ribatet, M., Sauquet, E., Gr ésillon, J.-M., Ouarda, T.B., 2007. Usefulness of the reversible jump
537 Markov chain Monte Carlo model in regional flood frequency analysis. Water Resources Research,
538 43(8). https://doi.org/10.1029/2006WR005525

Rigby, R.A., Stasinopoulos, D.M., 2005. Generalized additive models for location, scale and shape. Appl. Statist., 54(3): 507-554. https://doi.org/10.1111/j.1467-9876.2005.00510.x

Salas, J.D. (1992) Analysis and Modeling of Hydrologic Time Series. In: Maidment, D.R., Ed., Handbook of Hydrology, McGraw-Hill, New York, 19.1-19.72.

Scarf, P., 1992. Estimation for a four parameter generalized extreme value distribution. Communications in Statistics-Theory and Methods, 21(8): 2185-2201. https://doi.org/10.1080/03610929208830906

Sklar, M., 1959. Fonctions de repartition an dimensions et leurs marges. Publications de l'Institut Statistique de l'Universit éde Paris, 8: 229-231.

Su, C., Chen, X., 2018. Assessing the effects of reservoirs on extreme flows using nonstationary flood frequency models with the modified reservoir index as a covariate. Advances in Water Resources. https://doi.org/10.1016/j.advwatres.2018.12.004

Viglione, A., Merz, R., Salinas, J.L., Blöschl, G., 2013. Flood frequency hydrology: 3. A Bayesian analysis. Water Resources Research, 49(2): 675-692. https://doi.org/10.1029/2011WR010782

Villarini, G. et al., 2009. Flood frequency analysis for nonstationary annual peak records in an urban drainage basin. Advances in Water Resources, 32(8): 1255-1266. https://doi.org/10.1016/j.advwatres.2009.05.003

Wang, W. et al., 2017. Nonlinear filtering effects of reservoirs on flood frequency curves at the regional scale. Water Resources Research, 53(10): 8277-8292. https://doi.org/10.1002/2017WR020871

Wyżga, B., Kundzewicz, Z.W., Ruiz-Villanueva, V., Zawiejska, J., 2016. Flood generation mechanisms and changes in principal drivers, Flood Risk in the Upper Vistula Basin. Springer, pp. 55-75. https://doi.org/10.1007/978-3-319-41923-7_4

Xiong, B., Xiong, L., Chen, J., Chong-Yu, X., Li, L., 2018. Multiple causes of nonstationarity in the Weihe annual low-flow series. Hydrology and Earth System Sciences, 22(2): 1525. https://doi.org/10.5194/hess-22-1525-2018

Xiong, L., Jiang, C., Xu, C.Y., Yu, K.X., Guo, S., 2015. A framework of change-point detection for multivariate hydrological series. Water Resources Research, 51(10): 8198-8217. https://doi.org/10.1002/2015WR017677

Yan, L., Xiong, L., Liu, D., Hu, T., Xu, C.Y., 2017. Frequency analysis of nonstationary annual maximum flood series using the time-varying two-component mixture distributions. Hydrological Processes, 31(1): 69-89. https://doi.org/10.1002/hyp.10965

570 Zhang, Q., Gu, X., Singh, V.P., Xiao, M., Chen, X., 2015. Evaluation of flood frequency under
571 non-stationarity resulting from climate indices and reservoir indices in the East River basin, China.
572 Journal of Hydrology, 527: 565-575. https://doi.org/10.1016/j.jhydrol.2015.05.029

Hydrol. Earth Syst. Sci. Discuss., https://doi.org/10.5194/hess-2019-42
Manuscript under review for journal Hydrol. Earth Syst. Sci.
Discussion started: 19 March 2019

Hydrology and Earth System Sciences
Discussions

Tables

Table 1. The NGEV models with different formula of the location and scale parameters for flood frequency analysis.

Model	ID	The formula of distribution parameters	
		μ_t	$\ln(\sigma_t)$
NGEV(μ_t~*1*, σ_t~*1*)	M0	μ_0	σ_0
NGEV(μ_t~RI, σ_t~*1*)	M11	μ_0+ μ_1RI	σ_0
NGEV(μ_t~*1*, σ_t~RI)	M12	μ_0	σ_0+ σ_1RI
NGEV(μ_t~RI, σ_t~RI)	M13	μ_0+ μ_1RI	σ_0+ σ_1RI
NGEV(μ_t~RRCI, σ_t~*1*)	M21	μ_0+ μ_1RRCI	σ_0
NGEV(μ_t~*1*, σ_t~RRCI)	M22	μ_0	σ_0+ σ_1RRCI
NGEV(μ_t~RRCI, σ_t~RRCI)	M23	μ_0+ μ_1RRCI	σ_0+ σ_1RRCI

Hydrol. Earth Syst. Sci. Discuss., https://doi.org/10.5194/hess-2019-42
Manuscript under review for journal Hydrol. Earth Syst. Sci.
Discussion started: 19 March 2019

Hydrology and Earth System Sciences
Discussions

579 Table 2. The information of the reservoirs in the Hanjiang River basin.

Reservoirs	Longitude	Latitude	Area (km^2)	Year	Capacity (10^9 m^3)
Shiquan	108.05	33.04	23400	1974	0.566
Ankang	108.83	32.54	35700	1992	3.21
Huanglongtan	110.53	32.68	10688	1978	1.17
Dangjiangkou	111.51	32.54	95220	1967	21.0
Dangjiangkou+	111.51	32.54	95220	2010	13.0
Yahekou	112.49	33.38	3030	1960	1.32

580

581

582

Hydrol. Earth Syst. Sci. Discuss., https://doi.org/10.5194/hess-2019-42
Manuscript under review for journal Hydrol. Earth Syst. Sci.
Discussion started: 19 March 2019

Hydrology and Earth System Sciences
Discussions

584 Table 3. The change in the mean and standard deviation of AMDF after the construction of the
585 two large reservoirs (i.e., the Danjiangkou reservoir built by 1966, and the Ankang reservoir built by
586 1992).

Stations	Mean (m^3/s)			Standard deviation (m^3/s)		
	1956-1966	1967-1991	1992-2015	1956-1966	1967-1991	1992-2015
AK	9451	10468	6506	4341	4623	4454
HJG	14951	7524	4139	7896	5482	4074
HZ	16603	10120	5958	8833	5420	4721

587
588
589
590
591
592
593

Hydrol. Earth Syst. Sci. Discuss., https://doi.org/10.5194/hess-2019-42
Manuscript under review for journal Hydrol. Earth Syst. Sci.
Discussion started: 19 March 2019

Hydrology and Earth System Sciences
Discussions

Table 4. Correlation coefficients between the RRCI and the AMDF.

Subset of rainfall variables	AK			HJG			HZ		
	Pearson	Kendall	Spearman	Pearson	Kendall	Spearman	Pearson	Kendall	Spearman
-*	-0.36	-0.22	-0.29	-0.56	-0.42	-0.55	-0.53	-0.40	-0.53
M	-0.29	-0.28	-0.38	-0.67	-0.53	-0.74	-0.46	-0.38	-0.51
I	-0.34	-0.28	-0.37	**-0.78**	-0.64	-0.84	-0.55	-0.42	-0.57
V	-0.34	-0.28	-0.39	-0.67	-0.54	-0.75	-0.58	-0.47	-0.65
T	-0.12	-0.17	-0.24	-0.68	-0.55	-0.73	-0.49	-0.41	-0.58
M, *I*	-0.43	-0.29	-0.40	-0.72	-0.62	-0.82	-0.55	-0.42	-0.57
M, *V*	-0.45	-0.29	-0.41	-0.67	-0.55	-0.75	-0.55	-0.46	-0.62
M, *T*	-0.38	-0.25	-0.35	-0.69	-0.59	-0.79	-0.63	-0.47	-0.64
I, *V*	-0.50	-0.33	-0.44	-0.72	-0.63	-0.82	-0.65	-0.51	-0.68
I, *T*	-0.39	-0.25	-0.34	-0.75	**-0.65**	**-0.84**	-0.68	-0.50	-0.66
V, *T*	-0.46	-0.28	-0.39	-0.70	-0.58	-0.79	-0.69	-0.52	-0.70
M, *I*, *V*	-0.55	-0.33	-0.44	-0.69	-0.63	-0.83	-0.63	-0.47	-0.64
M, *I*, *T*	-0.45	-0.28	-0.39	-0.70	-0.63	-0.82	-0.67	-0.50	-0.66
M, *V*, *T*	-0.54	-0.31	-0.41	-0.67	-0.58	-0.78	-0.67	-0.50	-0.67
I, *V*, *T*	-0.53	-0.31	-0.41	-0.70	-0.64	-0.83	**-0.71**	**-0.53**	**-0.70**
M, *I*, *V*, *T*	**-0.55**	**-0.33**	**-0.44**	-0.67	-0.62	-0.82	-0.69	-0.51	-0.68

*The values in the first row are the correlation coefficients between RI and flood seires

Hydrol. Earth Syst. Sci. Discuss., https://doi.org/10.5194/hess-2019-42
Manuscript under review for journal Hydrol. Earth Syst. Sci.
Discussion started: 19 March 2019

Hydrology and Earth System Sciences
Discussions

598 Table 5. Results of copula models.

Stations	Scheduling-related variables	Pairs	Copula type	Parameters θ_c	Kendall's tau	Goodness-of-fit test based on the empirical copula	
						CvM*	p-value
AK	*M*, *I*, *V*, *T*	14	Clayton	0.06	0.03	0.108	0.965
		13	Clayton	0.47	0.19		
		12	Clayton	0.27	0.12		
		24|1	Frank	1.13	0.12		
		23|1	Frank	-1.8	-0.19		
		34|12	Clayton	0.1	0.05		
HJG	*I*, *T*	24	Clayton	0.95	0.32	0.624	0.755
HZ	*I*, *V*, *T*	24	Gumbel	1.07	0.07	0.107	0.95
		23	Clayton	0.58	0.22		
		34|2	Clayton	0.27	0.12		

599 * CvM is the statistic of the Cramer-von Mises test; if the p-value of the C-vine copula model is less than the significance level of 0.05, the model is considered to be
600 not consistent with the empirical copula.

601

602

Hydrol. Earth Syst. Sci. Discuss., https://doi.org/10.5194/hess-2019-42
Manuscript under review for journal Hydrol. Earth Syst. Sci.
Discussion started: 19 March 2019

Hydrology and Earth System Sciences
Discussions

603 Table 6. The selection of the GEV models and the significance of the final model with the chi-

604 square test.

Model ID	AK			HJG			HZ		
	AIC	Chi-square test		AIC	Chi-square test		AIC	Chi-square test	
		D	p-value		*D*	p-value		*D*	p-value
M0	1189.7	19.44	0.000	1158.9	64.17	0.000	1220.0	45.94	0.000
M11	1182.4	12.12	0.000	1155.7	60.95	0.000	1214.5	40.50	0.000
M12	1191.6	21.34	0.000	1155.8	61.10	0.000	1218.2	44.19	0.000
M13	1184.5	14.25	0.000	1149.4	54.69	0.000	1207.0	32.98	0.000
M21	1170.9	0.62	0.433	1146.8	52.10	0.000	1198.9	24.91	0.000
M22	1191.6	21.39	0.000	1138.2	43.50	0.000	1201.7	27.66	0.000
M23	**1170.3**	0.00	1.000	**1094.7**	0.00	1.000	**1174.0**	0.00	1.000

605

Hydrol. Earth Syst. Sci. Discuss., https://doi.org/10.5194/hess-2019-42
Manuscript under review for journal Hydrol. Earth Syst. Sci.
Discussion started: 19 March 2019

Hydrology and Earth System Sciences
Discussions

606 Table 7. The results of the parameter estimation for the best model (M23).

Station	μ_t	σ_t	ξ_0
AK	8323-5060RRCI	exp(8.353-0.508RRCI)	-0.065
HJG	12180-1053RRCI	exp(9.283-2.107RRCI)	0.006
HZ	11850-8937RRCI	exp(9.007-1.418RRCI)	-0.065

607

608

Hydrol. Earth Syst. Sci. Discuss., https://doi.org/10.5194/hess-2019-42
Manuscript under review for journal Hydrol. Earth Syst. Sci.
Discussion started: 19 March 2019

Hydrology and Earth System Sciences
Discussions

609 Table 8. The top 5 floods and the corresponding RRCI, $P_{MRI}^{\vee}$ and scheduling-related rainfall

610 variables after the construction (1967) of Danjiangkou reservoir in the HZ station.

Year	AMDF (m^3/s)	Values (Ranking in 1967-2015)					
		RRCI	RI	$P_{MRI}^{\vee}$	I	V	T
1983	25600	0.176 (3)	0.301 (-)	0.474 (3)	20.2 (1)	121.4 (19)	281 (2)
1975	19900	0.247 (6)	0.299 (-)	0.552 (6)	9.6 (18)	163.6 (13)	277 (6)
1974	18200	0.246 (5)	0.299 (-)	0.551 (5)	12.0 (7)	120.4 (20)	278 (4)
2005	16800	0.372 (12)	0.318 (-)	0.631 (11)	8.2 (27)	179.7 (10)	278 (4)
1984	16100	0.164 (1)	0.301 (-)	0.460 (2)	9.9 (15)	256.3 (4)	273 (9)

611

612

Hydrol. Earth Syst. Sci. Discuss., https://doi.org/10.5194/hess-2019-42
Manuscript under review for journal Hydrol. Earth Syst. Sci.
Discussion started: 19 March 2019

613 # Figures

614 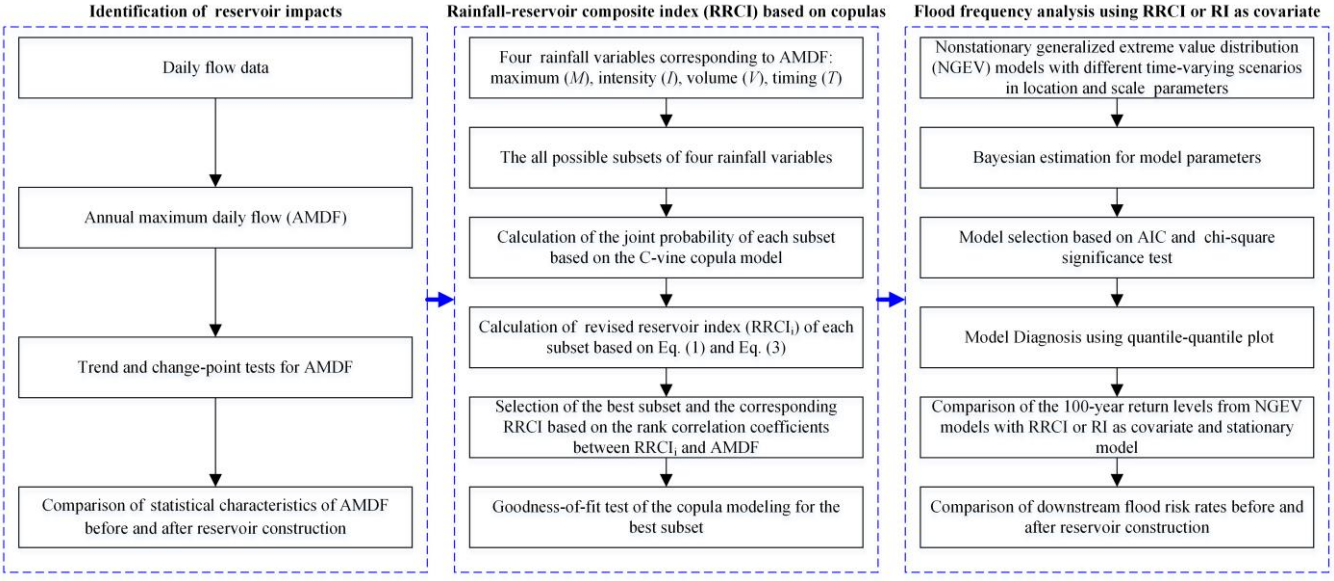

615 Figure 1. The flowchart of nonstationary flood frequency analysis with a rainfall-reservoir
616 composite index (RRCI).

617

Hydrol. Earth Syst. Sci. Discuss., https://doi.org/10.5194/hess-2019-42
Manuscript under review for journal Hydrol. Earth Syst. Sci.
Discussion started: 19 March 2019

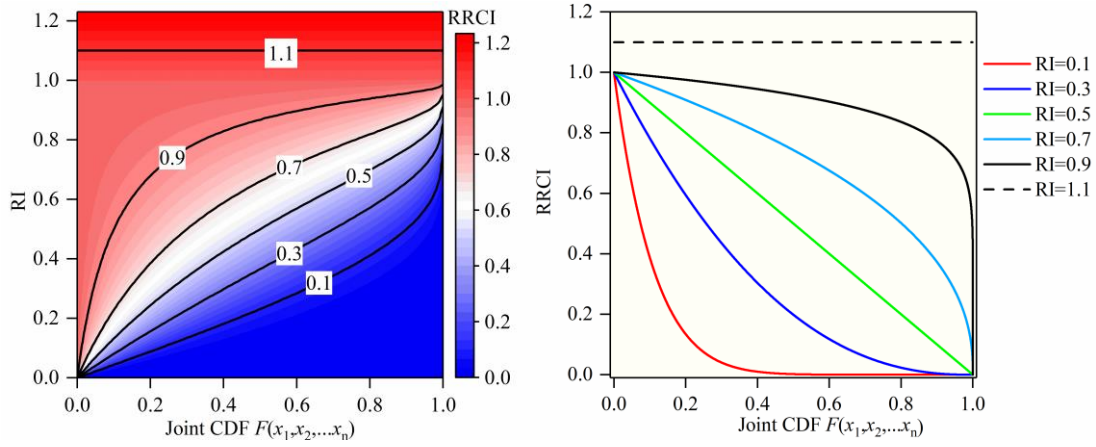

Figure 2. The relationship in the Eq. (3). The left panel is the contour of RRCI; the right panel is the F-RRCI curves under the different values of RI.

Hydrol. Earth Syst. Sci. Discuss., https://doi.org/10.5194/hess-2019-42
Manuscript under review for journal Hydrol. Earth Syst. Sci.
Discussion started: 19 March 2019

Hydrology and Earth System Sciences
Discussions

624

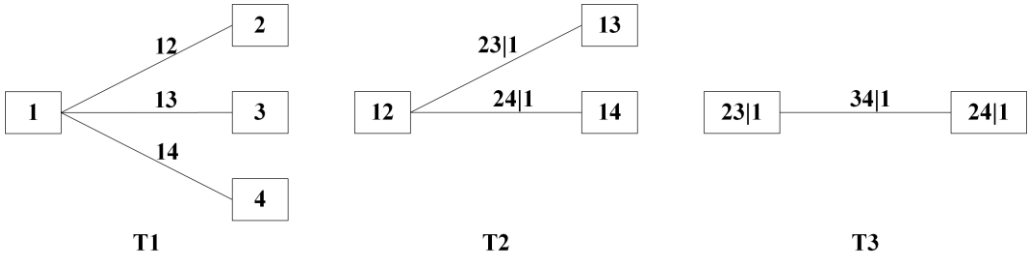

625 Figure 3. Decomposition of a C-vine copula with four variables and 3 trees (denoted by T1, T2

626 and T3).

627

628

Hydrol. Earth Syst. Sci. Discuss., https://doi.org/10.5194/hess-2019-42
Manuscript under review for journal Hydrol. Earth Syst. Sci.
Discussion started: 19 March 2019

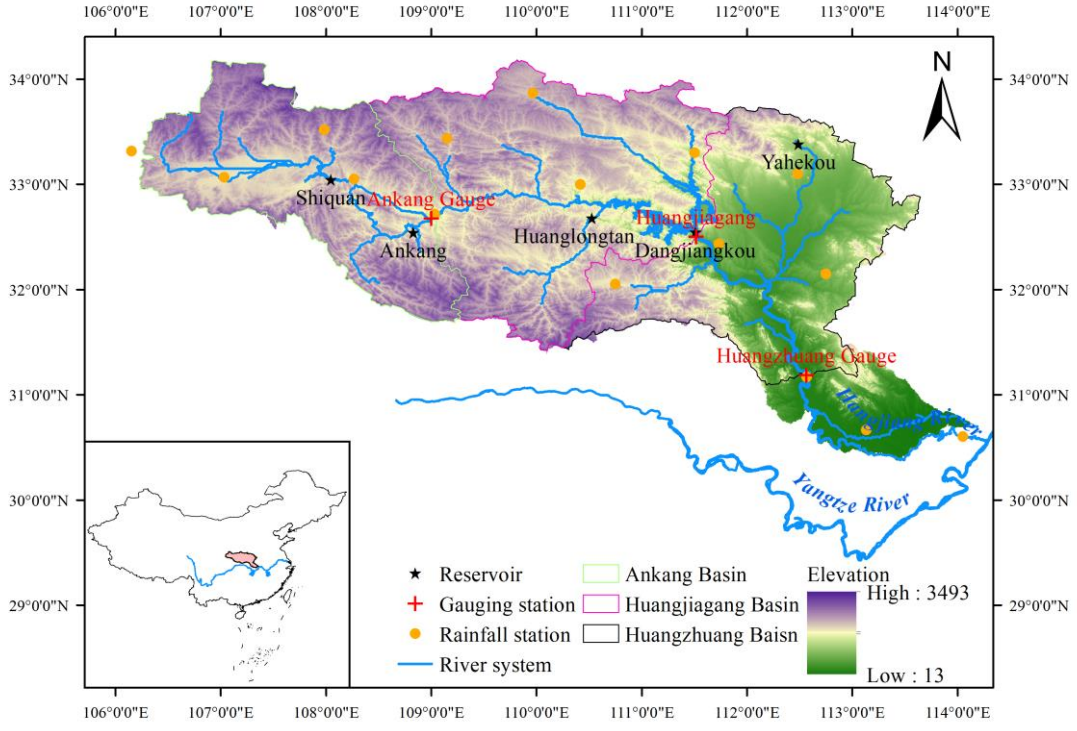

Figure 4. Geographic location of the reservoirs, gauging stations and rainfall stations in the Hanjiang River.

Hydrol. Earth Syst. Sci. Discuss., https://doi.org/10.5194/hess-2019-42
Manuscript under review for journal Hydrol. Earth Syst. Sci.
Discussion started: 19 March 2019

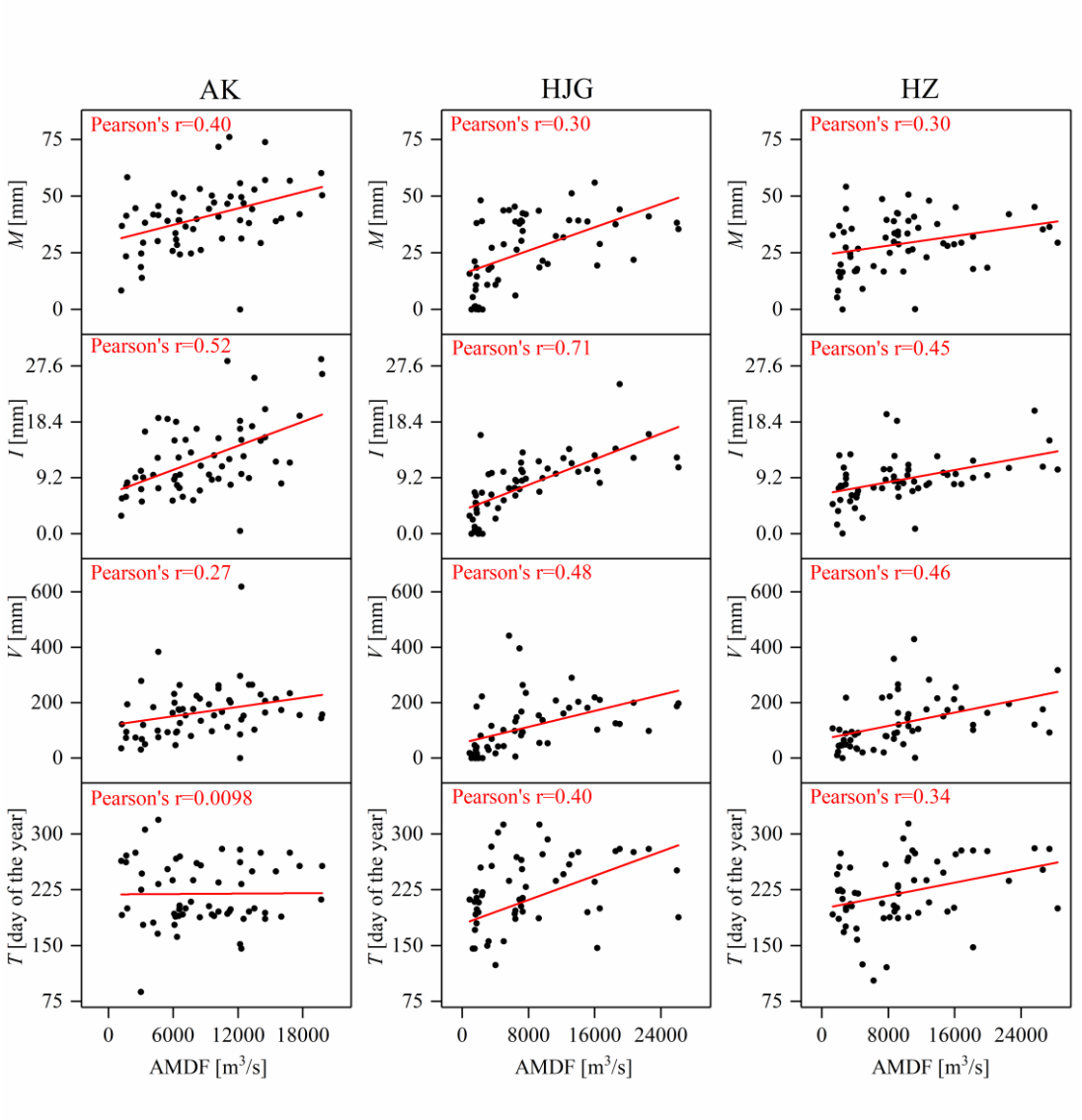

Figure 5. Linear correlation between the variables of multivariate MRI and AMDF.

Hydrol. Earth Syst. Sci. Discuss., https://doi.org/10.5194/hess-2019-42
Manuscript under review for journal Hydrol. Earth Syst. Sci.
Discussion started: 19 March 2019

639

640

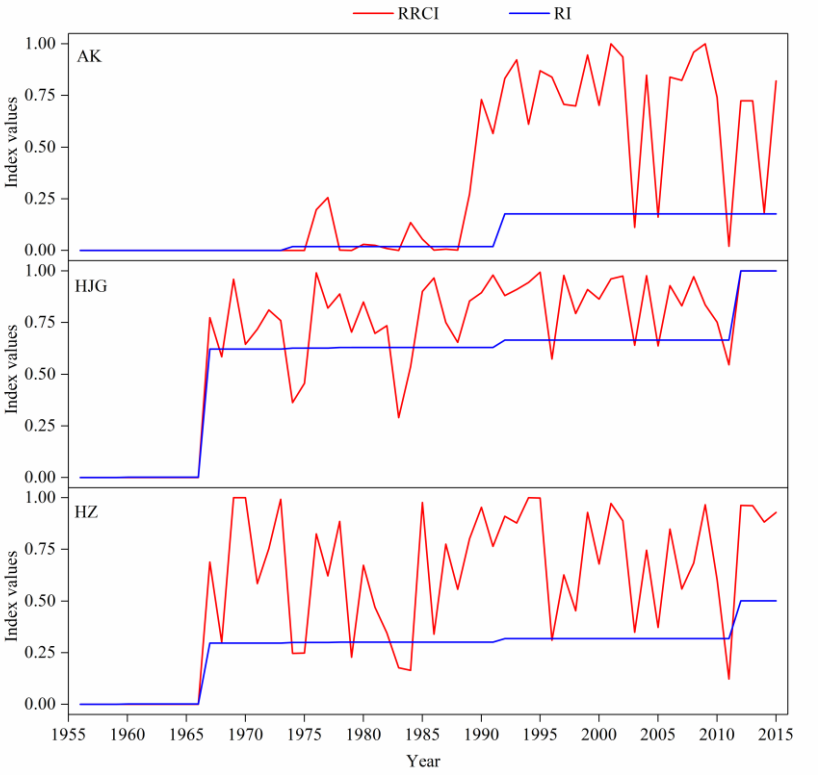

641

642 Figure 6. Variation of RI and RRCI.

643

Hydrol. Earth Syst. Sci. Discuss., https://doi.org/10.5194/hess-2019-42
Manuscript under review for journal Hydrol. Earth Syst. Sci.
Discussion started: 19 March 2019

Hydrology and Earth System Sciences
Discussions

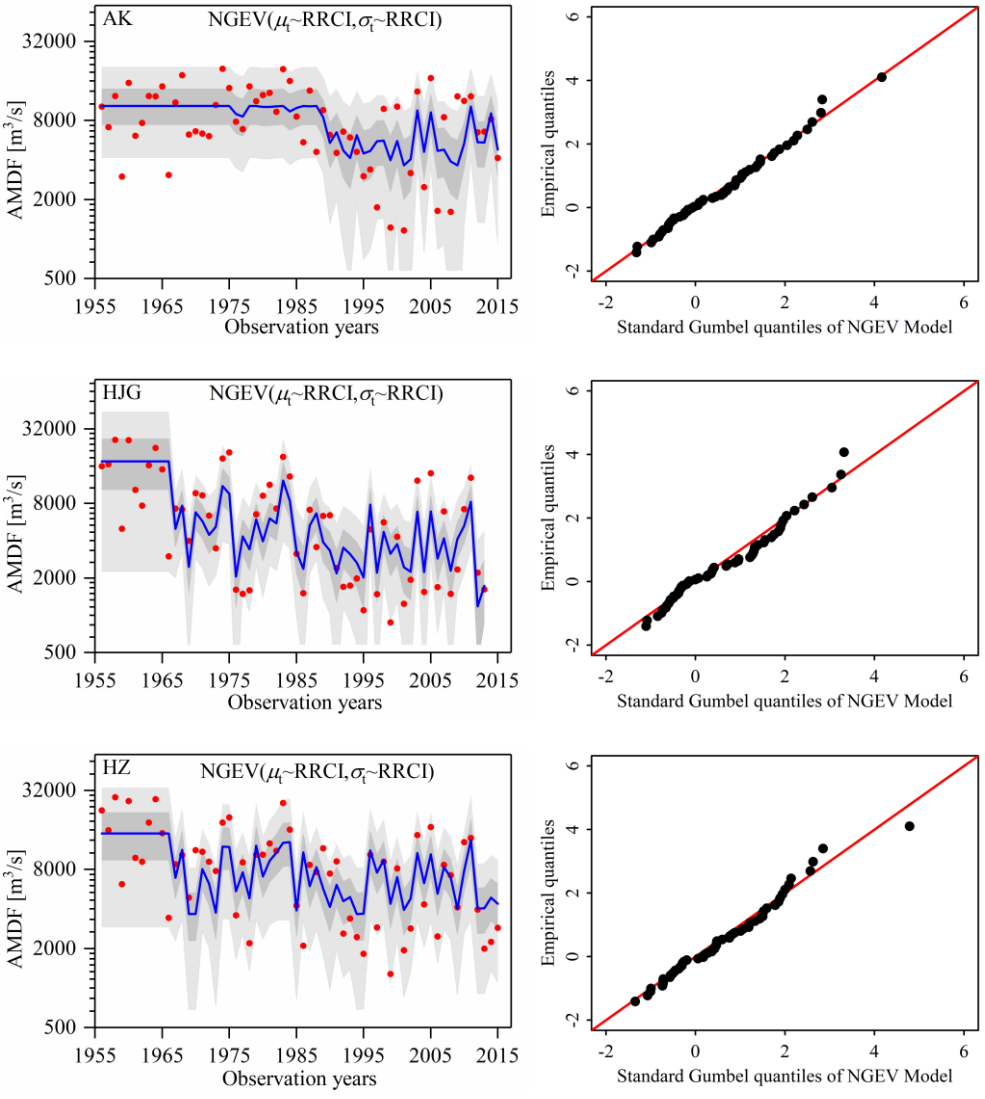

Figure 7. The performance of the best model (M23) for the Ankang (AK), Huangjiagang (HJG) and Huangzhuang (HZ) stations. The left panel is the centile curves plots (the 50th centile curves are indicated by thick blue; the light gray-filled areas are between the 5th and 95th centile curves; the dark grey-filled areas are between the 25th and 75th centile curves; the filled red points indicate the observed

651 series). The right panel is the quantile-quantile plots based on Eq. (15); a reasonable model should have

652 the plotted points close to 1:1 line.

653

Hydrol. Earth Syst. Sci. Discuss., https://doi.org/10.5194/hess-2019-42
Manuscript under review for journal Hydrol. Earth Syst. Sci.
Discussion started: 19 March 2019

654

655

656

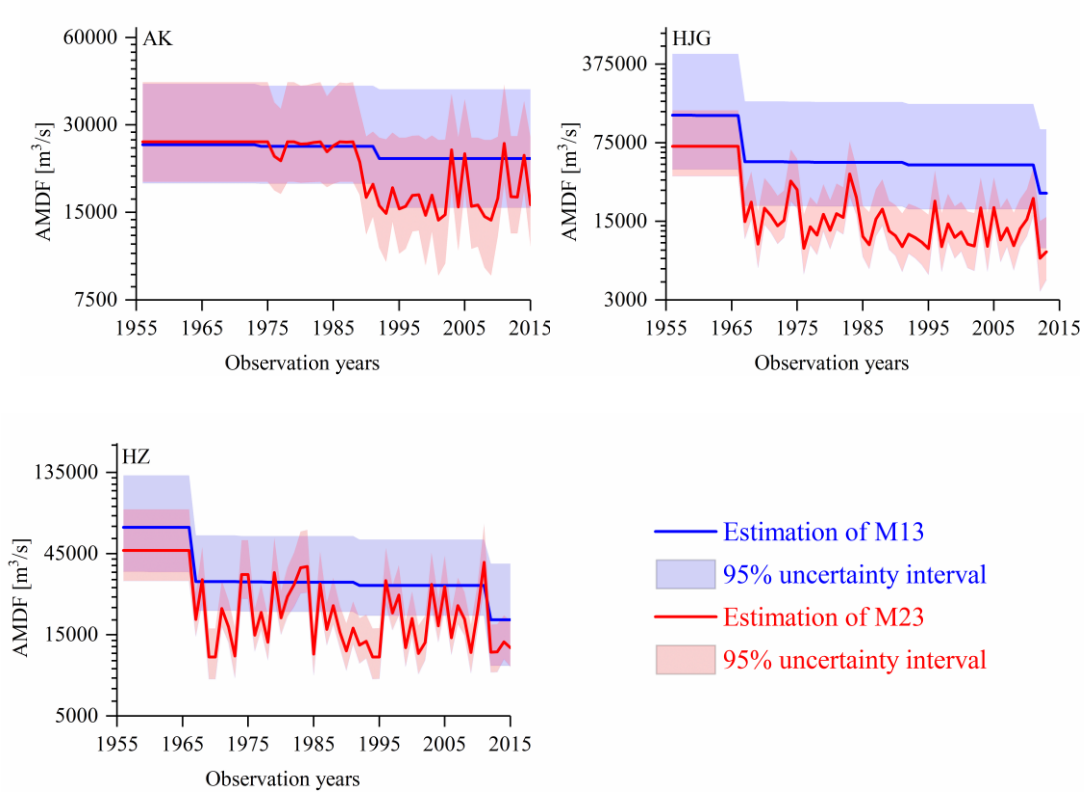

657 Figure 8. Statistical inference of the 100-year return levels from the models (M13 and M23) with the 95%

658 uncertainty interval.

659

Hydrol. Earth Syst. Sci. Discuss., https://doi.org/10.5194/hess-2019-42
Manuscript under review for journal Hydrol. Earth Syst. Sci.
Discussion started: 19 March 2019

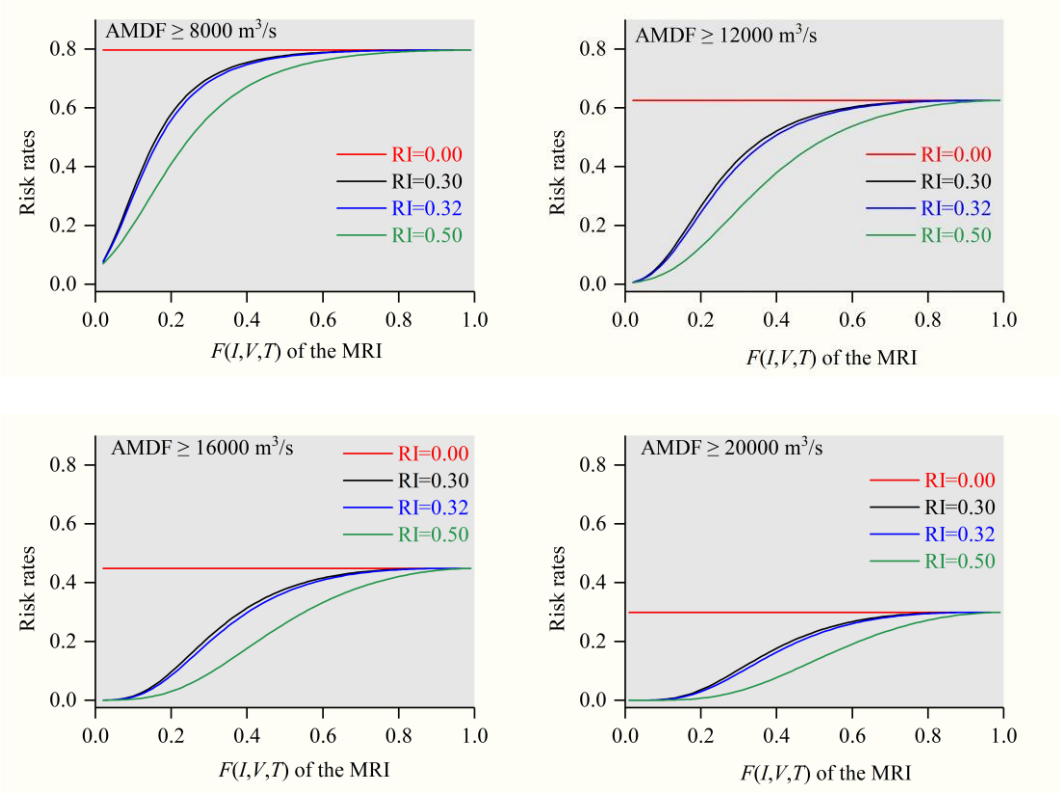

Figure 9. Comparison of risk rates of flood events corresponding to different levels of loss in the HZ station between 1956-1966 (RI=0), 1967-1992 (RI=0.30), 1992-2012 (RI=0.32), and 2013-future (RI=0.50) periods based on the final model (M23).